Tracer-kinetic model-driven registration improves data-driven tumour sub-segmentation of DCE-MRI data

G. A. Buonaccorsi[1], C. Roberts[1], J. P. O'Connor[1], C. J. Rose[1], S. Cheung[1], Y. Watson[1], A. Jackson[2], G. C. Jayson[3], and G. J. Parker[1]
[1]ISBE, University of Manchester, Manchester, United Kingdom, [2]WMIC, University of Manchester, Manchester, United Kingdom, [3]Cancer Research UK Dept of Medical Oncology, Christie Hospital, Manchester, United Kingdom

Introduction Parameters derived from quantitative dynamic contrast enhanced MRI (DCE-MRI) are increasingly used to support early decisions on the viability of emerging anti-angiogenic agents[1]. Standard practice[2] is to report statistics for a target tissue volume of interest (VOI), e.g. whole tumour median $IAUC_{60}$ or K^{trans}. It may be beneficial to more fully exploit the available information by using the spatially- and temporally-heterogeneous information in the 3-D parametric maps. One possible approach is tumour sub-segmentation, but it is necessary to first reduce motion-corruption in the DCE time series[3]. We present the results of using tracer-kinetic model-driven registration[4,5] (TKMDR) for motion correction prior to cross-visit tumour sub-segmentation.

Data We obtained 6 DCE-MRI scans from each of 10 patients enrolled in a clinical trial of a VEGF inhibitor antibody (bevacizumab)[6]: 2 scans within 7 days before treatment and 4 after (4 hours, then 2, 8 and 12 days). At each visit we acquired 3-D spoiled gradient echo (SPGR) images on a Philips 1.5 T Intera scanner for baseline T_1 estimation by the Variable Flip Angle (VFA) method[7] (3 acquisitions with flip angles of 2°, 10° and 30°; used to convert MR signal to contrast agent concentration for cross-visit normalisation) and for DCE-MRI (75 acquisitions: flip angle 20°, temporal resolution 4.97 s, voxel matrix 128 x 128 x 25). Omniscan (Amersham Health) was injected as a single bolus (dose 0.1 mmol/kg) after the 5th dynamic image, at a rate of 3 ml/s using a power injector. We manually defined tumour VOIs in 3-D on co-localised T_1- and T_2-weighted image volumes. All patients had liver metastases from colorectal primary tumours. All tumours had moderate or severe breathing-related motion. For each patient we analysed only the largest tumour.

Pat	1	2	3	4	5	6	7	8	9
Pre	2	4	6	4	7	3	4	6	1
Post	2	4	4	2	4	4	2	3	2

Table 1 Registration altered data structure as shown by the change in the number of PCs retained by the broken stick method[11].

Methods TKMDR aligns each DCE image to a time-point-matched synthetic target image[4]. We first used FLIRT[8] to register each VFA image to the first pre-contrast TKMDR target image, to improve the alignment of the baseline T_1 maps to the time series, then we used standard TKMDR to register the time-series images. In all cases we restricted transformations to 3D-translations[4]. We evaluated each time point registration based on the translation magnitudes and on the summed cross-correlation (Σcc) between adjacent images in the post-bolus phase of the DCE time series[5] (from the 20th time point onwards; i.e. 70 s to 280 s after contrast agent injection). For any time point with unfeasibly large translations or low Σcc, we visually compared the pre- and post-registration tumour locations with the VOIs. On finding poor registrations we either reverted to the pre-registration time point image or removed the time point completely (if the tumour was also misaligned in the original image).

After TKMDR we performed tumour sub-segmentation[3] using: cross-visit normalisation of DCE-MRI signal intensities by conversion to contrast agent concentrations *[CA](t)*, pooling data from each visit tumour VOI for the given patient, imputing missing/unphysiological *[CA](t)* values by iterative principal components analysis[9] (PCA), reducing dimensionality also by PCA, detecting and rejecting outlier *[CA](t)* series via a robust Mahalanobis distance that used the Minimum Covariance Determinant (MCD) estimator[10] and clustering by *k*-means (k = 7 to reflect tumour enhancing rim/non-enhancing core/surrounding liver and all partial volume combinations—alternative arrangements are clearly possible).

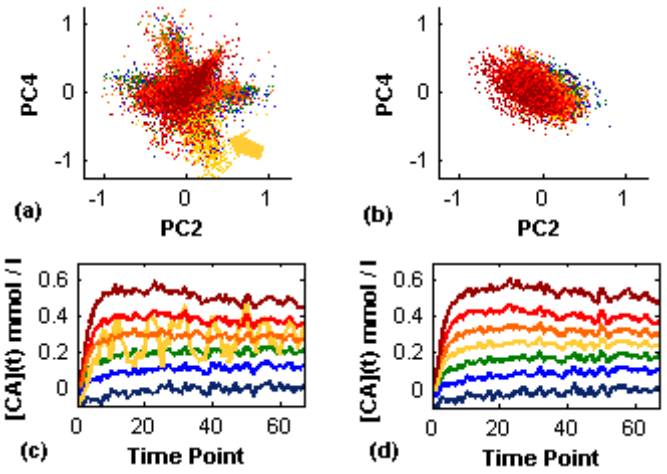

Fig 1 Scatterplots of PC2 v PC4 showed a lobular data structure before registration (a) that was resolved by TKMDR (b). Cluster 4 (yellow) was localised to the arrowed lobe before registration (b)—its class mean *[CA](t)* had the oscillating structure typical of breathing motion (c). This structure was also resolved by TKMDR (d). Note that the dot colours in (a) and (b) match the line colours in (c) and (d) and the colour map of Fig. 2.

Results One data set was not evaluable after TKMDR (>15 time points required reversion or rejection at each visit). For 8 of the remaining 9 tumours TKMDR gave a statistically-significant reduction in Σcc by the Wilcoxon Signed Rank Test (non-parametric equivalent to paired *t*-test). The number of principal components (PCs) retained for dimensionality reduction decreased after TKMDR in 5 tumours and increased in 2 (Table 1). Registration reduced data structure in the PC space and removed an atypical cluster mean *[CA](t)* (Fig. 1) corresponding to a cluster that was present at only 1 visit before registration (Fig. 2). The segmentation is reproducible (the pre-treatment visits are similar) and sensitive to local changes after treatment, especially from day 2 onwards where higher enhancing clusters (higher label numbers) reduce in volume.

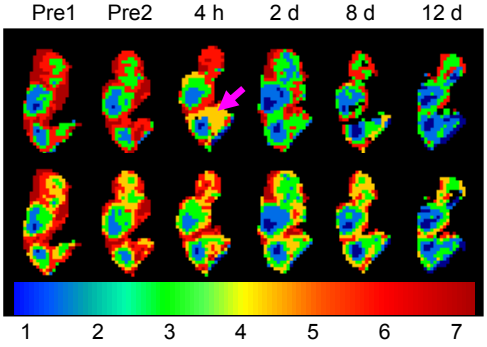

Fig 2 Tumour sub-segmentation maps. Cluster 4 (yellow) was primarily localised to visit 3 (4 h) before registration (top row, arrowed) but more uniformly distributed among the visits after TKMDR (bottom row). Clusters had integer labels 1 to 7 indicating low to high overall mean *[CA](t)* using the colour map shown—the colour-coding matches Fig. 1.

Discussion For a typical bolus injection DCE time series, *[CA](t)* changes rapidly only in the first-pass and recirculation phases. The reduced Σcc showed that TKMDR increased cross-correlations between adjacent late time points, implying a reduction in motion corruption. The first PC is the projection in a data space that maximises variance and thereby signal (by assumption, signal outweighs noise). Higher order PCs must be orthogonal to the first so the lobular PC structure of Fig 1a implies that at least one noise source was of comparable strength to the dominant signal. As TKMDR removed this lobular structure (Fig 1b) its most likely cause was motion corruption—the elimination by TKMDR of the cluster with the oscillating mean *[CA](t)* (Fig 1c and 1d) supports this hypothesis. Detailed motion patterns will be specific to a single visit so the localisation of the removed cluster to visit 3 (Fig 2) and the smoother variation in the post-TKMDR cluster spatial distribution are also consistent with the removal of motion corruption. Note that the atypical pre-registration cluster could have been interpreted as evidence of an acute treatment-induced effect, and we conclude that registration and careful data examination are necessary to avoid such potential pitfalls.

Conclusions Motion in DCE time series data can have a significant and damaging effect on cluster structure when using data-driven tumour sub-segmentation methods. We have shown that such motion effects can be corrected using tracer-kinetic model-driven registration.

References 1. Leach MO *et al.* Br J Cancer **92**:1599(2005). 2. Evelhoch JL *et al.* Clin Cancer Res **10**:3650(2004). 3. Buonaccorsi GA *et al.* Lect Notes Comp Sci **6363**:121(2010). 4. Buonaccorsi GA *et al.* Magn Reson Med **58:**1010(2007). 5. Caunce A *et al.* Proc ISMRM:**16**:3130(2008). 6. O'Connor JPB *et al.* Clin Cancer Res **15**:6674(2009). 7. Fram E *et al.* Magn Reson Img **5**:201(1987). 8. Jenkinson M *et al.* Neuroimage **17**:825(2002). 9. Stanimirova I *et al.* Talanta **72**:172 (2007). 10. Rousseeuw PJ, van Zomeren BC. J Am Stat Assoc **85**:633(1990). 11. Joliffe IT. *Principal Components Analysis.* Springer, NY (2002).

Acknowledgments *This project was partially-funded by CRUK grant C237/A6295 and by Genentech Inc., San Francisco, CA.*